# ELECTROCHEMICAL STUDIES ON THE SYNTHESIS AND CHARACTERIZATION OF LITHIUM AND VANADIUM AND CHROMIUM PHOSPHATE COMPOUNDS

**A. A.El-Aziz[1], Atef Y. Shenouda[1], M.M.S. Sanad[1], H. F. Y. Khalil[2] and M. M. B. El-Sabbah[2]**

[1]*Central Metallurgical R & D Institute (CMRDI), Tebbin, P. O. Box: 87 Helwan, Egypt.*
[2]*Chemistry Department Faculty of Science, Al-Azhar University, Nasr City, Egypt.*

## ABSTRACT

*The use of monodiphosphate compounds as renewable sources of energy as positive (cathode) material for lithium-ion batteries (LIB) is considered a great target. Lithium vanadium chromium monodiphosphate (LVCPP)$Li_9V_{2.8}Cr_{0.2}(P_2O_7)_3(PO_4)_2$ and the Na-doped:$Li_{8.75}Na_{0.25}V_{2.8}Cr_{0.2}(P_2O_7)_3(PO_4)_2$ (LNVCPP) compounds have been prepared by using the sol-gel method. The prepared materials are characterized by XRD, FESEM, and EDX. The XRD data is indicated the presence of a single-phase of $Li_9V_{2.8}Cr_{0.2}$ $(P_2O_7)_3(PO_4)_2$ and $Li_{8.75}Na_{0.25}V_{2.8}Cr_{0.2}(P_2O_7)_3(PO_4)_2$ with trigonal structure. Both cycle performance and rate capability have shown improvement with moderate Na doping content. $Li_9V_{2.8}Cr_{0.2}(P_2O_7)_3(PO_4)_2$ and $Li_{8.75}Na_{0.25}V_{2.8}Cr_{0.2}(P_2O_7)_3(PO_4)_2$ compounds presented the good electrochemical rate and cyclic ability. The cell is prepared with x=0.25 delivered a specific discharge capacity of 50 mAhg$^{-1}$ after 35 cycles in comparison with the other sample. The enhancement of the rate and cyclic capability may be attributed to the optimizing particle size, morphologies, and structural stability with the proper amount of Na-doping (x =0.25) in Li sites.*

*Keywords:*

Lithium-ion battery, Cathode material, Sol-gel, and $Li_{8.75}Na_{0.25}V_{2.8}Cr_{0.2}(P_2O_7)_3(PO_4)_2$.

## 1. INTRODUCTION

The demand in high energy density of lithium-ion batteries has enhanced small electronics devices during the past two decades[1]. In order to face the requirements of these lithium -ion battery technologies, many attempts were made to prepare electrode materials that can easily intercalate and transfer Li-ions at appropriate or suited potentials and a variety of oxides and polyanionic materials have been reported [2–4]. After dealing with monoclinic $Li_3V_2(PO_4)_3$ (LVP), which includes higher specific energy than lithium iron phosphate (LFP), vanadium oxy phosphates and vanadium phosphates are gaining substantial attention as a substitute positive material for lithium-ion batteries [2,5–8]. For example, monoclinic $Li_3V_2(PO_4)_3$ can deliver a theoretical capacity of 197 mAh g$^{-1}$ when the three Li ions are extracted at the average potential of about 4.1 V[9,10]. As recommended by Goodenough and his coworkers, the previous described material worked at a higher potential in comparison to their iron equivalent due to the inductive impact between the phosphate groups and vanadium[5]. This leads to increase the specific capacity. However, monoclinic LVP faces some problems from a great drop in structural instability and electronic conductivity with severe delithiation at high potentials[10]. This makes the extraction of the 3$^{rd}$ lithium ion unfeasible, consequently limiting the specific capacity to 131 mAhg$^{-1}$[11]. On further exploration, a new class of the novel layered monodiphosphate, $Li_9V_3(P_2O_7)_3(PO_4)_2$ was used as potential positive materials for Li-ion batteries[12]. $Li_9V_3(P_2O_7)_3(PO_4)_2$ has suitable layered structure and facile lithium diffusion. The theoretical capacity of $Li_9V_3(P_2O_7)_3(PO_4)_2$ is 173.5 mAh g$^{-1}$ with six Li ions per formula extracted along the ab-plane or c-axis,–related to V$^{3+}$/V$^{5+}$ redox couples. Furthermore, allocated to the inductive effect of diphosphate radicals $P_2O_7$ and monophosphate radicals $PO_4$ in the framework, $Li_9V_3(P_2O_7)_3(PO_4)_2$ can display higher redox potential and good electrochemical stability during charge/ discharge. This kind of material displays a

capacity of 110 mAh g$^{-1}$ and good cycle performance after 30 cycles over a broad operating voltage range of 2.0–4.6 V[13,14]. This new polyanionic compounds, with a twofold inner symmetry presents in the layered structure, provided rich and interesting crystal chemistry information on the electrochemical recrystallization during charge and discharge process. Although this material exhibited good capacity and reversibility after 30 cycles and may be expected to be used as another alternative cathode materials[12]. It is assumed that there are some unexplored places still exist at the doping of V site in $Li_9V_3(P_2O_7)_3(PO_4)_2$ systems, which influence on the structural and electrochemical properties. Inspired by these considerations, it has been sought to study the effect of part substitution of Cr in V site on the structural and electrochemical properties of the $Li_9V_3$ $(P_2O_7)_3(PO_4)_2$ compounds. It is anticipated that Cr doping may allow the formation of more stable phase and improve the electrical or ionic conductivity, which would enhance the electrochemical properties, including improved specific capacity at a high rate and better or excellent cycle-life performance. The doped $Li_9V_{3-x}Cr_x$ $(P_2O_7)_3(PO_4)_2$ compounds were synthesized by using the sol-gel method as reported for the 1$^{st}$ time [15]. The nine Li-ions occupy three different Li sites per molecular formula in $Li_9V_3(P_2O_7)_3(PO_4)_2$ as the following ($Li_1$(2b), $Li_2$(4d), and $Li_3$(12g)), and Li ions in site $Li_1$(2b) with the lowest formation enthalpy first extraction from the layered structure at ~3.7 V vs. Li [13,14,16–20]. If the Li ions in $Li_1$(2b) site are substituted by other steady alkali metal ions, the voltage plateau at ~3.7 V will be faded and only the voltage plateau at ~4.5 V left. If so, the charge and corresponding discharge voltage will be much improved. Taking into consideration there are six Li ions in $Li_3$(12g) site, which can carry out the oxidation of $V^{3+}$ to $V^{5+}$, thus the theoretical capacity is nearly unchanged after the substitution. Therefore, the energy density of $Li_9V_3(P_2O_7)_3(PO_4)_2$ can be enhanced due to the analysis of this material design. It was reported that Na ions were used to substitute the Li ions in $Li_1$(2b) site, since the atomic radius of Na-ion is close to that of Li-

ion in all alkali metal ions[13]. Furthermore, the layered structure of $Li_9V_3(P_2O_7)_3(PO_4)_2$ could become unstable after extreme Li-ion extraction exactly like that of $LiCoO_2$ [21], and the vanadium ($V^{4+}/V^{5+}$) in Li-extracted vanadium based phosphates, such as $Li_{5-x}V(PO_4)_2F_2$, $Li_{1-x}VP_2O_7$ and $Li_{3-x}V_2(PO_4)_3$, are readily dissolved in the electrolyte [22–24]. $Li_8NaV_3(P_2O_7)_3(PO_4)_2$ and $Li_9V_3(P_2O_7)_3(PO_4)_2$ with layered structure may be more-appropriate as positive electrodes for rechargeable Li-batteries, and the Li intercalation behaviors of several phosphate cathode materials (such as $Li_3V_2(PO_4)_3$ and $LiFePO_4$) were investigated as well [25,26]. Therefore, the Li intercalation properties of $Li_9V_3(P_2O_7)_3(PO_4)_2$ were compared and presented with that of $Li_8NaV_3(P_2O_7)_3(PO_4)_2$ [27]. The aim of this work is the study of introduce of a small ratio of Na like $Na_{0.25}$ that can be used to replace Li-ions. Therefore, preparation and characterization of the $Li_9V_{2.8}Cr_{0.2}$ $(P_2O_7)_3(PO_4)_2$ and $Li_{8.75}Na_{0.25}V_{2.8}Cr_{0.2}(P_2O_7)_3$ - $(PO_4)_2$ compounds. According to the best of our knowledge, there is no work devoted $Li_{8.75}Na_{0.25}V_{2.8}Cr_{0.2}(P_2O_7)_3(PO_4)_2$ vs. $Li_9V_{2.8}Cr_{0.2}$ $(P_2O_7)_3(PO_4)_2$ as materials obtained by sol-gel method.

## 2. EXPERIMENTAL

### 2.1. Synthesis and characterization

$Li_9V_{2.8}Cr_{0.2}$ $(P_2O_7)_3(PO_4)_2$ and $Li_{8.75}Na_{0.25}$-$V_{2.8}Cr_{0.2}(P_2O_7)_3(PO_4)_2$ samples for lithium-ion batteries were prepared by the sol-gel method. The solution for sol-gel method was obtained by dissolving stoichiometric ratios of lithium hydroxide (LiOH.H$_2$O, Sigma-Aldrich, >98.5%), sodium bicarbonate (NaHCO$_3$, Sigma-Aldrich,>99%), ammonium metavana-date (NH$_4$VO$_3$, Sigma-Aldrich,> 99%), chromium nitrate (Cr(NO$_3$)$_3$·9H$_2$O, Sigma Aldrich,>99%), and ammonium dihydrogen phosphate (NH$_4$H$_2$PO$_4$, Sigma-Aldrich,>99%) in distilled water and mixed well with citric acid in distilled water. The resulting precursor solution was evaporated at 80 °C under constant stirring to yield the gel. The gel was further heated until dryness and decomposition of the organic matter. After that the precursor powder was ground, then transferred into a tube

furnace and heated at 400°C for 3 h under air atmosphere. After cooling to room temperature, the powder was ground again, and sintered at 800 °C for 7 h under flowing of mixed gas 95%Ar + 5%H$_2$. To reduce the crystallite size and particle size, ball milling of the as-synthesized LVCPP and LNVCPP was carried out for different time intervals.

X-ray diffraction (XRD) patterns for materials were collected on a Brucker axis D8 diffractometer with crystallographic data software Topas 2 using Cu-Kα ($\lambda$= 1.5406 nm) radiation operating at 40 kV and 30 mA. The angle scan rate was set at 2 °/min. The microstructure and morphology of the samples were characterized by Field emission electron microscope (FE-SEM QUANTAFEG 250). EDX was carried out by SEM, JEOL model JSM5040 and Inductive Coupled Plasma (ICP) with Perkin Elmer Optima 2000 DV.

## 2.2. Electrochemical measurements

The working electrodes (WE) for electrochemical measurements were manufactured by mixing the synthesized Li$_9$V$_{2.8}$Cr$_{0.2}$ (P$_2$O$_7$)$_3$(PO$_4$)$_2$ and Li$_{8.75}$Na$_{0.25}$V$_{2.8}$Cr$_{0.2}$(P$_2$O$_7$)$_3$(PO$_4$)$_2$ active materials with carbon black and polyvinylidene difluoride (PVDF) in the ratio of 80:10:10 wt.%. Typically, the slurry was prepared by mixing all the components in presence of N-methyl pyrrolidone (NMP) as a solvent. Then, the aluminum disk substrate (1 cm$^2$ area) was coated with this slurry to form the WE. The active material loading onto each electrode was approximately 5 mg cm$^{-2}$. After being dried at 70 °C under vacuum overnight, the electrodes were transferred to an Ar-filled glove box with H$_2$O and O$_2$ content <1 ppm. The electrochemical measurements performed in coin cells where metallic Li (Sigma Aldrich, >99.9%) acted as a counter and a reference electrode. Celgard® C300 (microporous polypropylene) as a separator and 1 M LiPF$_6$ in EC: DMC (1:1, vol.%) were used as an electrolyte. The electrochemical capacity measurements were performed in the voltage range between 2 and 4.6 V and the electrochemical capacity of samples was

evaluated using a Bitrode battery tester. Furthermore, electrochemical impedance spectroscopy measurements were applied using frequency range between 10$^6$ and 10$^{-2}$ Hz at amplitude of 10 mV using Potentiostat Model Parastat Princeton 4000.

## 3. RESULTS AND DISCUSSION

### 3.1. Material characterization

The XRD patterns of the Li$_9$V$_{2.8}$Cr$_{0.2}$ (P$_2$O$_7$)$_3$(PO$_4$)$_2$ and Li$_{8.75}$Na$_{0.25}$V$_{2.8}$Cr$_{0.2}$(P$_2$O$_7$)$_3$-(PO$_4$)$_2$ samples are shown in Fig.1. The two samples are found to be a single-phase with trigonal structure and no impurity phases can be detected under the resolution of our XRD instrument. Our results are in a good agreement with the reported one for LVCPP [28]. It is observed that a small amount substitution of Cr$^{3+}$ for V$^{3+}$ ions in a six-fold coordination environment, the whole diffraction peak positions almost kept consistently with Cr content. This can be explained in the light of the similarity between the ionic radii of Cr$^{3+}$ and V$^{3+}$ ions: $r_{Cr}3+ = 0.615$Å and $r_V3+ = 0.640$ Å, respectively[15,29]. Also, the absence of diffraction peaks of impurities suggests that the final products are compounds of a single phase, indicating that doping a low amount of Na$^+$ as compared by the amount of Li$^+$ does not significantly affect the single structure of Li$_{8.75}$Na$_{0.25}$V$_{2.8}$Cr$_{0.2}$(P$_2$O$_7$)$_3$(PO$_4$)$_2$.

Also, the slightly change in peak position with the increase of Na content and the cell volumes of Na-doped Li$_{8.75}$Na$_{0.25}$V$_{2.8}$Cr$_{0.2}$-(P$_2$O$_7$)$_3$(PO$_4$)$_2$ samples are somewhat larger than that of pristine one. Furthermore, the substitution of smaller radius of Li$^+$ ($r = 0.73$ Å) by larger Na$^+$ ($r = 1.13$ Å) may be responsible for the variation. Larger cell volume could supply the larger channel for transport of Li$^+$ and facilitate rapid diffusion of Li$^+$ in particles of the active materials, in favor of improving the electrochemical performance [27,30]. Furthermore, the crystallite size is calculated from Scherer equation[31]:

$$L = \frac{0.94\lambda}{\beta \cos \theta} \quad .........................................(1)$$

Where; $L$ is the crystallite size, $\lambda$ is the wavelength of the target (1.5406 Å for Cu), $\beta$ is full width half maximum (FWHM) and $\theta$ is the chosen diffraction angle. The calculated crystallite size values are around 52 nm, while for $x=0.25$, the value is 40 nm. It is observed that 0.25 Na substitution to LCVPP gives a less crystallite size
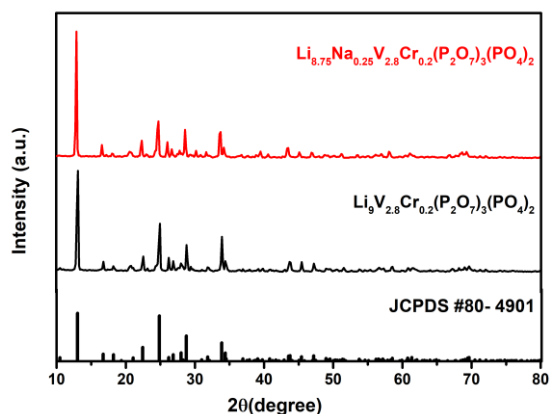
FESEM images of the samples are recorded in Fig. 2. The morphology of $Li_9V_{2.8}Cr_{0.2}(P_2O_7)_3(PO_4)_2$ compound is dense agglomerated in the structure with a particle size of 400 to 600 nm. The addition of $Na_x$ with $x=0.25$ to polyanion phosphate changes the dense aggregated crystal into a spherical small particle size of 300 to 400 nm as shown in Fig.2(b) along with the formation of nanowires. Therefore, it can be observed that the $Na_{0.25}$ substitution for Li in $Li_9V_{2.8}Cr_{0.2}(P_2O_7)_3(PO_4)_2$ material can reduce the grain size and facilitate the generation of $Li_{8.75}Na_{0.25}V_{2.8}Cr_{0.2}(P_2O_7)_3(PO_4)_2$ micro wires and spheres. Similar results were reported by Kuang et. al. for $Li_8Na_{1.0}V_{2.8}Cr_{0.2}(P_2O_7)_3(PO_4)_2$[27].



**Fig.1 X-ray diffraction (XRD) patterns for $Li_{9-x}Na_xV_{2.8}Cr_{0.2}(P_2O_7)_3(PO_4)_2$ ($x = 0.0$ and 0.25).**
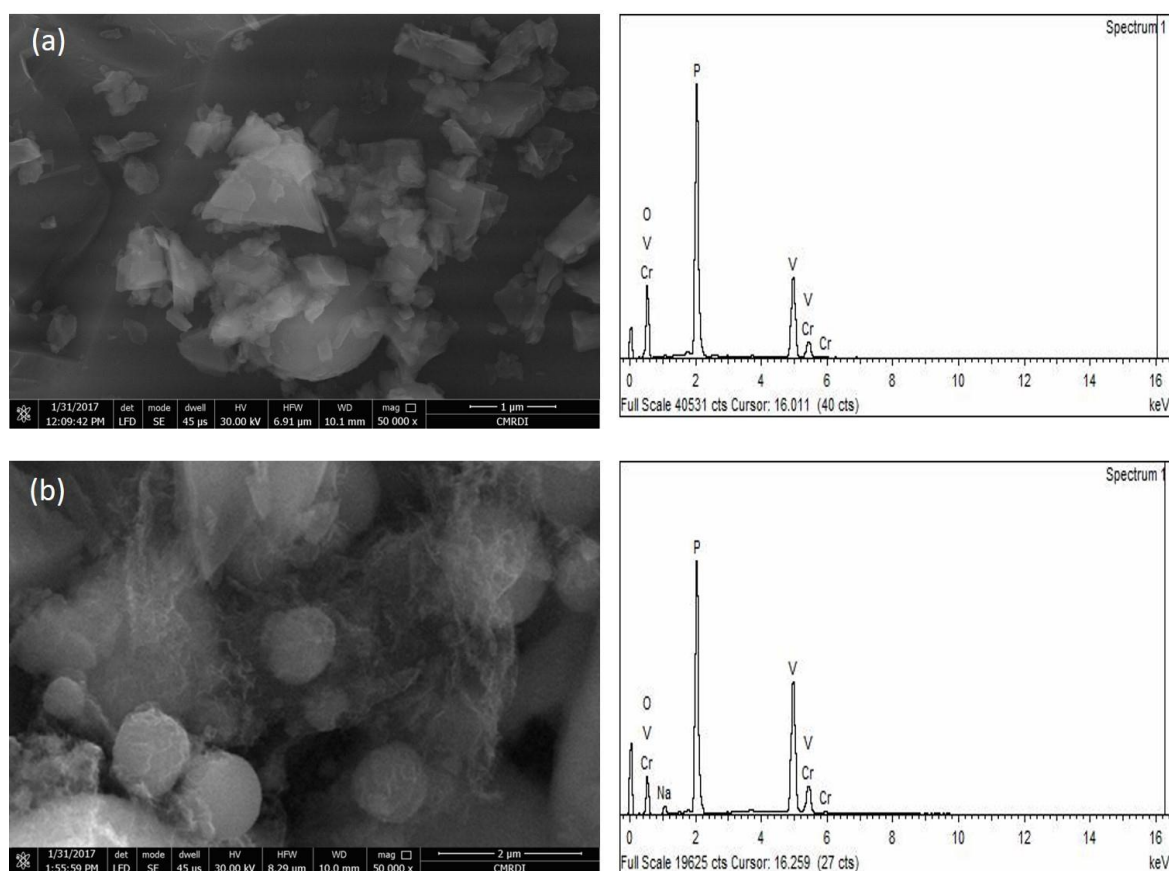


**Fig. 2 FESEM images and EDX spectra of $Li_{9-x}Na_xV_{2.8}Cr_{0.2}(P_2O_7)_3(PO_4)_2$ particles with different Na doping levels, x = 0.0 to 0.25 from (a) to (b), respectively.**

The chemical composition of the samples is analyzed by energy dispersive x-ray spectra (EDX) as shown in Fig. 2 and inductive coupled plasma (ICP) analysis. The results are recorded in Tables 1 and 2. ICP has more accurate analysis than EDX for the stoichiometric ratios of the elements in the samples.

## 3.2. Electrochemical characterization

### 3.2.1. Electrochemical Impedance spectra

Electrochemical impedance spectra (EIS) measurements are done for the samples pellets of dimensions: radius ($r$) ~0.5 cm and thickness ($t$) ~0.2 cm to measure the bulk resistance of the materials as shown in Fig. 3. The resistance, resistivity, and conductivity of the material of the sample are listed in Table 3. It is observed that the lowest resistance and resistivity besides the highest conductivity are obtained for the pellet prepared from the $Li_{8.75}Na_{0.25}VCrPP$ compound.

On the other hand, the electrochemical impedance spectra measurements are also carried out to have more information about the lithium-ion diffusion of $Li_9V_{2.8}Cr_{0.2}(P_2O_7)_3(PO_4)_2$ and $Li_{8.75}Na_{0.25}V_{2.8}Cr_{0.2}(P_2O_7)_3$-$(PO_4)_2$ for the cells. Fig. 4 shows the Nyquist plots of $Li_9V_{2.8}Cr_{0.2}(P_2O_7)_3(PO_4)_2$ and $Li_{8.75}Na_{0.25}V_{2.8}Cr_{0.2}(P_2O_7)_3$-$(PO_4)_2$ in the cells after one cycle at 0.2 C (theoretical capacity), when the cell materials are fully activated with keeping their open circuit voltages stable (around 3.0 V) after rest for several hours.

**Table 1. Element analysis of $Li_{9-x}Na_xV_{2.8}Cr_{0.2}(P_2O_7)_3(PO_4)_2$ where x=0.0 and 0.25, materials by ICP.**

| Compounds | Li% | Na% | V% | Cr% | P% | O%[*] | Molecular formula |
|---|---|---|---|---|---|---|---|
| $Li_9V_{2.8}Cr_{0.2}(P_2O_7)_3(PO_4)_2$ | 6.8 | 0 | 16.2 | 1.06 | 26.3 | 49.64 | $Li_{9.01}V_{2.94}Cr_{0.18}P_{7.87}O_{28.79}$ |
| $Li_{8.75}Na_{0.25}V_{2.8}Cr_{0.2}(P_2O_7)_3(PO_4)_2$ | 6.56 | 0.62 | 15.6 | 1.18 | 26.54 | 48.98 | $Li_{8.76}Na_{0.26}V_{2.86}Cr_{0.21}P_{8.01}O_{28.65}$ |

- O % was calculated by subtraction from 100%

**Table 2. Element analysis of $Li_{9-x}Na_xV_{2.8}Cr_{0.2}(P_2O_7)_3(PO_4)_2$, where x=0.0 and 0.25 materials by EDX. * * Li % was calculated by subtraction from 100%**

| Compounds | Li%[**] | Na% | V% | Cr% | P% | O % | Molecular formula |
|---|---|---|---|---|---|---|---|
| $Li_9V_{2.8}Cr_{0.2}(P_2O_7)_3(PO_4)_2$ | 6.787 | 0 | 12.04 | 0.96 | 26.62 | 53.593 | $Li_{9.81}V_{2.73}Cr_{0.2}P_{8.5}O_{31.15}$ |
| $Li_{8.75}Na_{0.25}V_{2.8}Cr_{0.2}(P_2O_7)_3(PO_4)_2$ | 6.203 | 1.57 | 17.34 | 1.26 | 27.12 | 46.507 | $Li_{8.76}Na_{0.27}V_{2.8}Cr_{0.2}P_{7.22}O_{26.99}$ |

* * Li % was calculated by subtraction from 100%

**Table 3. The Resistance, resistivity, and conductivity of $Li_{9-x}Na_xV_{2.8}Cr_{0.2}(P_2O_7)_3(PO_4)_2$, where x=0.0 and 0.25 materials.**

| Compounds | Resistance($\Omega$) | Resistivity ($\Omega$.cm) | Conductivity(S.cm$^{-1}$) |
|---|---|---|---|
| $Li_9V_{2.8}Cr_{0.2}(P_2O_7)_3(PO_4)_2$ | 8480 | 33284 | $3.00 \times 10^{-5}$ |
| $Li_{8.75}Na_{0.25}V_{2.8}Cr_{0.2}(P_2O_7)_3(PO_4)_2$ | 6560 | 25748 | $3.88 \times 10^{-5}$ |
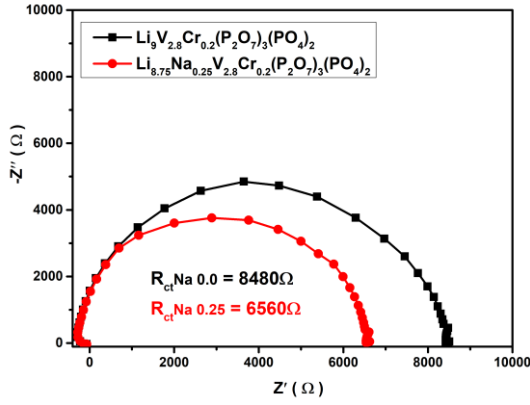
**Fig. 3 The Nyquist plot for $Li_{9-x}Na_xV_{2.8}Cr_{0.2}$ $(P_2O_7)_3(PO_4)_2$, $x = 0.0$ and 0.25 pellets.**

All the profiles exhibit a semicircle in the high frequency and a straight line in the low frequency. The high-frequency semicircle is related to the charge transfer process and the diameter of the semicircle is approximately equal to the charge transfer resistance ($R_{ct}$). The straight lines region at low frequencies represents the diffusion of the Li-ion in the electrolyte-electrode interface layer towards the bulk electrode materials. The $Li_{8.75}Na_{0.25}V_{2.8}$-$Cr_{0.2}$ $(P_2O_7)_3(PO_4)_2$ cells show the smallest $R_{ct}$, as evidenced by the smallest diameter of semicircle as shown in Fig. 4. All the impedance parameters of the different cells are given in Table 4. The diffusion coefficient values of the lithium ions in the bulk electrode materials are calculated using Eqs. (2 and 3) [32, 33]:

$$Z_{re} = R_e + R_{ct} + \sigma_w.\ \omega^{-0.5} \qquad (2)$$

$$D = 0.5(RT/An^2F^2\sigma_\omega C)^2 \qquad (3)$$

Where $D$ is the diffusion coefficient, $\sigma_w$ Warburg factor can be obtained through the linear fitting of the $Z`$ vs. $\omega^{-0.5}$ relationship within the low-frequency range, $R$ is the gas constant, $T$ is the absolute temperature, $F$ is the Faraday's constant, $A$ is the area of the electrode surface, $n$ is number of electron $Li^+$/Li, and $C$ is the molar concentration of $Li^+$ ions. It is indicated that $Li_{8.75}Na_{0.25}V_{2.8}Cr_{0.2}$ $(P_2O_7)_3(PO_4)_2$ has the lowest diffusion coefficient value of 7.14 x$10^{-11}$ cm$^2$/s. Fig. 5 indicates the plot of $Z_{re}$ or $Z`$ versus the reciprocal square root of the lower angular

frequencies, $\omega^{-0.5}$. The diffusion of the $Li^+$ ions is so-called Warburg diffusion [32,33]. This relation is governed by Eq. (2). Thereby, it is observed that the Warburg impedance coefficient, $\sigma_w$ is 442.49 $\Omega$ s$^{0.5}$ for $Li_{8.75}Na_{0.25}$-$V_{2.8}Cr_{0.2}(P_2O_7)_3(PO_4)_2$ which is the lowest value in comparison with the other samples, as shown in Fig.5.



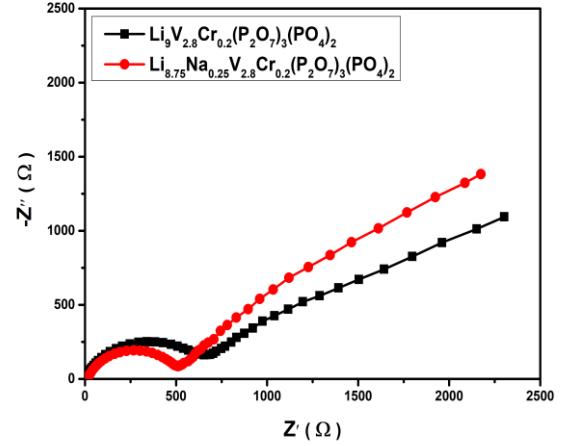**Fig. 4 The Nyquist plot for $Li_{9-x}Na_xV_{2.8}Cr_{0.2}$ $(P_2O_7)_3(PO_4)_2$ cells,x =0.0and 0.25.**
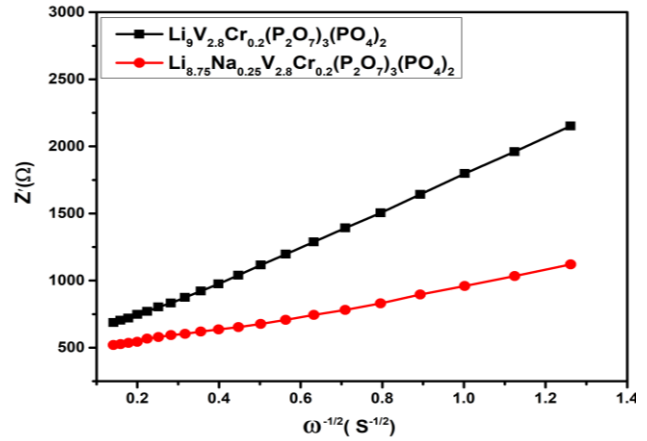


**Fig. 5. The relationship between Z′ and ω-0.5 for $Li_{9-x}Na_xV_{2.8}Cr_{0.2}$ $(P_2O_7)_3(PO_4)_2$, x = 0.0 and 0.25 samples.**

### 3.2.2. Potentiodynamic and galvanostatic measurements of the electrochemical cells

In order to investigate the electrochemical behavior of $Li_9V_{2.8}Cr_{0.2}$ $(P_2O_7)_3(PO_4)_2$ and $Li_{8.75}Na_{0.25}V_{2.8}Cr_{0.2}(P_2O_7)_3(PO_4)_2$ cells, cyclic voltammetry (CV) is carried out in the potential range of 2.0–4.6 V vs. $Li^+$ using a scanning rate

**Table 4. EIS parameters for different cells of $Li_{9-x}Na_xV_{2.8}Cr_{0.2}$ $(P_2O_7)_3(PO_4)_2$, where x=0.0 and 0.25.**

| Cells | Resistance of Electrolyte $R_s$ ($\Omega$) | Charge transfer Resistance $R_{ct}$ ($\Omega$) | Warburg impedance coefficient $\sigma_\omega$ ($\Omega \cdot s^{0.5}$) | Diffusion Coefficient D($cm^2$/s) | Double Layer Capacitance $C_{dl}$ (F) | Current Electrode/Electrolyte interferance $i°$(A) |
|---|---|---|---|---|---|---|
| $Li_9V_{2.8}Cr_{0.2}$ $(P_2O_7)_3(PO_4)_2$ | 5.50 | 648.60 | 1216.52 | $9.45 \times 10^{-12}$ | $1.94 \times 10^{-6}$ | $3.95 \times 10^{-5}$ |
| $Li_{8.75}Na_{0.25}V_{2.8}Cr_{0.2}$ $(P_2O_7)_3(PO_4)_2$ | 6.53 | 504.24 | 442.49 | $7.14 \times 10^{-11}$ | $1.99 \times 10^{-6}$ | $5.08 \times 10^{-5}$ |

of 0.1 mV.s$^{-1}$ and the results are presented in Fig.6. Three anodic peaks appeared during oxidation and are labeled as $a_1$, $a_2$ and $a_3$, while two cathodic peaks are denoted as $c_1$ and $c_2$ occurred during reduction. The potentials for the CV peaks of $Li_{9-x}Na_xV_{2.8}Cr_{0.2}$ $(P_2O_7)_3(PO_4)_2$ composites are listed in Table 5. The $Li_9V_{2.8}Cr_{0.2}(P_2O_7)_3(PO_4)_2$ cell exhibited three oxidation peaks for the following reactions:

$Li_9(V^{3+})_{2.8}Cr_{0.2}$ $(P_2O_7)_3(PO_4)_2 \longrightarrow Li_6(V^{4+})_{2.8}Cr_{0.2}$ $(P_2O_7)_3(PO_4)_2 + 3Li^+ + 3e^-$ (4)
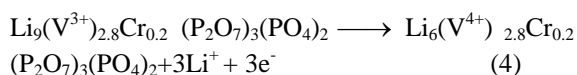
($E = 3.62$ V)

Eq. (4) has a potential for de-insertion of 3 Li-atom for the first phase during the charging process. The obtained potential is in agreement with the reported one, 3.6V [34]. Also, the oxidation of $Cr^{3+}$ to $Cr^{4+}$ gives a small peak at 3.7 V as follows:

$Li_6(V^{4+})_{2.8}(Cr^{3+})_{0.2}(P_2O_7)_3(PO_4)_2Li_{5.8} \longrightarrow (V^{4+})_{2.8}(Cr^{4+})_{0.2} P_2O_7)_3(PO_4)_2 + 0.2Li^+ + 0.2e^-$ (5)
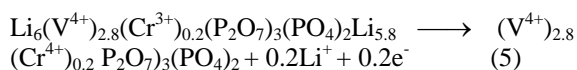
($E$=3.7 V)

The second phase of lithium deinsersion for another three atoms, takes place according to Eq. (6) beside the oxidation of $V^{4+}$ to $V^{5+}$. The peak observed at 4.1 V is in agreement with reported data [35]:

$Li_6(V^{4+})_{2.8}Cr_{0.2}$ $(P_2O_7)_3(PO_4)_2 \longrightarrow Li_3(V^{5+})_{2.8}Cr_{0.2}$ $(P_2O_7)_3(PO_4)_2 + 3Li^+ + 3e^-$ (6)
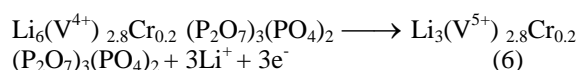
($E = 4.1$ V)

The reduction processes revealed three peaks at 4.49, 3.9 and 3.72 V as shown in Fig. 6. These peaks can be ascribed by the reduction of $V^{5+}/V^{4+}$ and $V^{4+}/V^{3+}$.

$Li_{8.75}Na_{0.25}V_{2.8}Cr_{0.2}$ $(P_2O_7)_3(PO_4)_2$ has the smallest anodic and cathodic potential difference peaks, implying that $Li_{8.75}Na_{0.25}V_{2.8}Cr_{0.2}$ $(P_2O_7)_3(PO_4)_2$ has the best reversibility and electrochemical performance, in accordance of this compound.
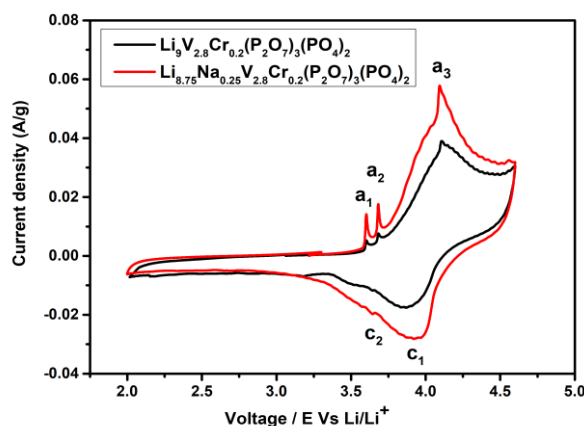


**Fig. 6. CVs of $Li_{9-x}Na_xV_{2.8}Cr_{0.2}$ $(P_2O_7)_3(PO_4)_2$, x = 0.0 and 0.25) cells ν=0.1 mV s$^{-1}$.**

*Table 5*. **Potentials for CV peaks of $Li_{9-x}Na_xV_{2.8}Cr_{0.2}$ $(P_2O_7)_3(PO_4)_2$, where x=0.0 and 0.25.**

| Samples | Anode $a_1$(v) | Anode $a_2$(v) | Anode $a_3$(v) | Cathode $c_1$(v) | Cathode $c_2$(v) |
|---|---|---|---|---|---|
| $Li_9V_{2.8}Cr_{0.2}$ $(P_2O_7)_3(PO_4)_2$ | 3.597 | 3.673 | 4.095 | 3.938 | 3.646 |
| $Li_{8.75}Na_{0.25}V_{2.8}Cr_{0.2}$ $(P_2O_7)_3(PO_4)_2$ | 3.601 | 3.676 | 4.100 | 3.877 | 3.630 |

Fig. 7 showed the specific charge-discharge capacity vs. voltage for the first cycle of the cells cycled at 0.05 C rate in the voltage range 2-4.8 V. There are three plateaus appeared in the charge at 3.65, 4 and 4.5 V and two plateaus appeared in the discharge process at 4.1 and 3.5 V, which are characterized the good electrochemical reactions between two phases and good agreement with the cyclic voltammetry analysis. It is observed that the 1st discharge capacity of $Li_{8.75}Na_{0.25}V_{2.8}Cr_{0.2}$ $(P_2O_7)_3(PO_4)_2$ gives 50 $mAhg^{-1}$. This cell delivers a greater capacity than the other cells.
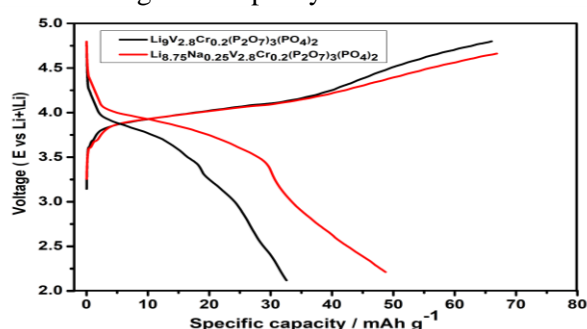


**Fig. 7. The voltage- capacity profile for $Li_{9-x}Na_xV_{2.8}Cr_{0.2}$ $(P_2O_7)_3(PO_4)_2$ , x = 0.0 and 0.25) samples.**

In order to investigate the effect of Na doping on the rate and cycle performance, $Li_9V_{2.8}Cr_{0.2}$ $(P_2O_7)_3(PO_4)_2$ and $Li_{8.75}Na_{0.25}V_{2.8}Cr_{0.2}(P_2O_7)_3(PO_4)_2$ cells are cycled between 2 and 4.8 V potential windows at various current densities as shown in Fig. 8. The total of 35 cycles of charge and discharge are made in the charge/discharge curves for every cell, and the charging/discharging current rate is increased from C/20 (theoretical capacity divided by 20 hours, i.e. charging/discharging current =173.5 mAh/g/20h) to 2 C (theoretical capacity divided by 0.5 hours, i.e. charging/discharging current = 173.5 mAh/g/0.5h) after every 5 cycles. In the first 5 cycles at a lower current rate C/20, from the cycle no.6 at a C/15 rate to the cycle no.30 at 2 C, the discharge capacity of doped phase $Li_{8.75}Na_{0.25}V_{2.8}Cr_{0.2}$ $(P_2O_7)_3(PO_4)_2$ becomes higher than that of undoped one, and as the current rate further decreases, the rate capability is enhanced remarkably in comparison with the undoped one. The result

indicates that the cycle-ability and rate performance of the lithium vanadium chromium polyphosphate can be enhanced by doping with Na. The improved electrochemical performance of the Na-doping sample is mainly related to the Li-ion transportation, good diffusion between the active materials and electrolyte and crystallite size of this compound.
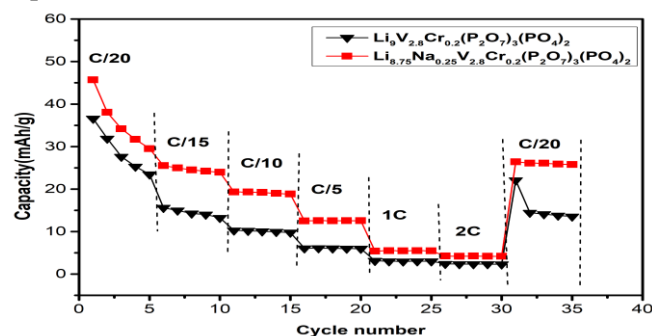


**Fig. 8. cycle life for specific discharge capacity performance of $Li_{9-x}Na_xV_{2.8}Cr_{0.2}$ $(P_2O_7)_3(PO_4)_2$, (x= 0.0 and 0.25) cells at various discharge rates in the voltage range of 2.0–4.8 V.**

**CONCLUSION**

$Li_9V_{2.8}Cr_{0.2}$ $(P_2O_7)_3(PO_4)_2$ and $Li_{8.75}Na_{0.25}V_{2.8}Cr_{0.2}(P_2O_7)_3(PO_4)_2$ have been successfully synthesized by the sol-gel method. The XRD results indicated that single-phase of $Li_9V_{2.8}Cr_{0.2}$ $(P_2O_7)_3(PO_4)_2$ and $Li_{8.75}Na_{0.25}V_{2.8}Cr_{0.2}(P_2O_7)_3(PO_4)_2$ materials with trigonal structure can be obtained. The electrochemical properties of $Li_9V_{2.8}Cr_{0.2}$ $(P_2O_7)_3(PO_4)_2$ and $Li_{8.75}Na_{0.25}V_{2.8}Cr_{0.2}$-$(P_2O_7)_3(PO_4)_2$ phases have been investigated, Furthermore, the EIS parameters have the Na-doped sample with $Na_{0.25}$. Also, the CV of the cell compound has higher density content among the other cells. The doping of Li sites by the proper amount of $Na^+$ would be favorable for structural stability of $Li_{9-x}Na_xV_{2.8}Cr_{0.2}(P_2O_7)_3(PO_4)_2$ where x=0.25 and thus can be counteracted the volume shrinking/swelling during the $Li^+$ reversible extraction/insertion resulting in the improvement of the cyclic ability. It is suggested that the partial substitution of Li with Na at *x* = 0.25 would be favorable for electrochemical performance and cyclic ability due to the enhancement of the structural stability of $Li_{9-x}Na_xV_{2.8}Cr_{0.2}$ $(P_2O_7)_3(PO_4)_2$

where x=0.25, thereby optimizing the particle size and shape.

## ACKNOWLEDGEMENT

## REFERENCES

[1] N.S. Choi, Z. Chen, S.A. Freunberger, X. Ji, Y.K. Sun, K. Amine, G. Yushin, L.F. Nazar, J. Cho, P.G. Bruce, Angew. Chemie - Int. Ed. 51 (2012) 9994–10024.

[2] C. Masquelier, L. Croguennec, Chem. Rev. 113 (2013) 6552–6591.

[3] M.G. Kim, J. Cho, Adv. Funct. Mater. 19 (2009) 1497–1514.

[4] L. FU, H. LIU, C. LI, Y. WU, E. RAHM, R. HOLZE, H. WU, Prog. Mater. Sci. 50 (2005) 881–928.

[5] A.K. Padhi, J. Electrochem. Soc. 144 (1997) 2581.

[6] S.-C. Yin, H. Grondey, P. Strobel, M. Anne, L.F. Nazar, J. Am. Chem. Soc. 125 (2003) 10402–10411.

[7] M.S. Whittingham, Y. Song, S. Lutta, P.Y. Zavalij, N. a. Chernova, J. Mater. Chem. 15 (2005) 3362.

[8] G. Hautier, A. Jain, T. Mueller, C. Moore, S.P. Ong, G. Ceder, Chem. Mater. 25 (2013) 2064–2074.

[9] H. Huang, S.-C. Yin, T. Kerr, N. Taylor, L.F. Nazar, Adv. Mater. 14 (2002) 1525–1528.

[10] X. Rui, Q. Yan, M. Skyllas-Kazacos, T.M. Lim, J. Power Sources 258 (2014) 19–38.

[11] P. Balasubramanian, M. Mancini, P. Axmann, Electrochem. Soc. 164 (2017) 6047–6053.

[12] Q. Kuang, J. Xu, Y. Zhao, X. Chen, L. Chen, Electrochim. Acta 56 (2011) 2201–2205.

[13] Q. Kuang, Y. Zhao, J. Xu, J. Phys. Chem. C 115 (2011) 8422–8429.

[14] Z. Liang, Y. Zhao, Electrochim. Acta 94 (2013) 374–380.

[15] J. Xu, Y. Zhao, Q. Kuang, Y. Dong, Electrochim. Acta 56 (2011) 6562–6567.

[16] X. Miao, C. Li, W. Chu, P. Wu, D.G. Tong, RSC Adv. 5 (2015) 243–247.

[17] G.F. Gu, D.M. Tang, P. Wu, H.Y. Tian, D.G. Tong, Mater. Lett. 92 (2013) 247–251.

[18] X. Lin, Y. Zhao, Q. Kuang, Z. Liang, D. Yan, X. Liu, Y. Dong, Solid State Ionics 259 (2014) 46–52.

[19] Q. Kuang, Y. Zhao, Electrochim. Acta 58 (2011) 296–302.

[20] Q. Kuang, Z. Lin, Y. Zhao, X. Chen, L. Chen, J. Mater. Chem. 21 (2011) 14760.

[21] H. Wang, J. Electrochem. Soc. 146 (1999) 473.

[22] Y. Makimura, L.S. Cahill, Y. Iriyama, G.R. Goward, L.F. Nazar, Chem. Mater. 20 (2008) 4240–4248.

[23] C. Wurm, M. Morcrette, G. Rousse, L. Dupont, C. Masquelier, Chem. Mater. 14 (2002) 2701–2710.

[24] A.R. Cho, J.N. Son, V. Aravindan, H. Kim, K.S. Kang, W.S. Yoon, W.S. Kim, Y.S. Lee, J. Mater. Chem. 22 (2012) 6556.

[25] N. Kalaiselvi, C.-H. Doh, C.-W. Park, S.-I. Moon, M.-S. Yun, Electrochem. Commun. 6 (2004) 1110–1113.

[26] X.H. Rui, N. Yesibolati, C.H. Chen, J. Power Sources 196 (2011) 2279–2282.

[27] Q. Kuang, Y. Zhao, Y. Dong, Q. Fan, X. Lin, X. Liu, J. Power Sources 306 (2016) 337–346.

[28] P. Balasubramanian, M. Mancini, P. Axmann, 164 (2017) 6047–6053.

[29] R.D. Shannon, Acta Crystallogr. Sect. A 32 (1976) 751–767.

[30] Q. Chen, X. Qiao, Y. Wang, T. Zhang, C. Peng, W. Yin, L. Liu, J. Power Sources 201 (2012) 267–273.

[31] H.K.L. Atef Y. Shenouda, J. Power Sources 185 (2008) 1386–1391.

[32] A.Y. Shenouda, H.K. Liu, J. Alloys Compd. 477 (2009) 498–503.

[33] A.Y. Shenouda, H.K. Liu, J. Electrochem. Soc. 157 (2010) A1183.

[34] R. Satish, V. Aravindan, W.C. Ling, S. Madhavi, J. Power Sources 281 (2015) 310–317.

[35] H.K.L. Atef Y. Shenouda, Electrochim. Acta 51 (2006) 5973–5981.

**الملخص العربي**

**الدراسات الكهروكيميائية على تحضير وتوصيف مركبات فوسفات اللثيوم والفانديوم والكروم**

يعتبر استخدام مركبات احادية وثنائية الفوسفات كمصادر للطاقة المتجددة كأقطاب موجبة في بطاريات ايون اللثيوم هدفا عظيما . تم تحضير مركبات اللثيوم فانديوم كروم احادي وثنائي الفوسفات المطعمة والغير مطعمة بالصوديوم بطريقة الـ sol-gel . تم عمل توصيف لهذه المركبات باستخدام حيود الأشعة السنية والمجهر الالكتروني الانبعاثي ومطيافية تشت السينية . من خلال تحليل حيود الأشعة السينية تبين ان هذه المركبات تحتوي علي طور واحد ذا هيكل ثلاثي . بعد اجراء عمليات الشحن والتفريغ للبطاريات المحتوية علي اقطاب موجبة من هذه المركبات تبين علي مدرا ٣٥ دورة شحن وتفريغ ومع تنوع في شدة التيار ان المركبات المطعمة بالصوديوم بنسبة (0.25) ذات اداء أفضل من الغير المطعمة . المركبات المطعمة بالصوديوم وصلت سعة التخزين الكهربي 50mGh/g ويرجع ذلك الي ثبات الهيكل والقدرة علي تخزين الطاقة بشكل افضل التي تتميز بها المركبات المطعمة بالصوديوم عن نظيرتها الغير مطعمة .